SPE 94252

Investigating Applicability of Vogel's IPR for Fractured Wells

J.I. Rueda,* SPE, A. Zakharov, SPE, and J. Mach, SPE, YUKOS E&P

* Now with Pinnacle Technologies

This paper was prepared for presentation at the 2005 SPE Production Operations Symposium held in Oklahoma City, Oklahoma, U.S.A., 17– 19 April 2005.

Abstract

It is a common practice in the oil industry that production engineers use Vogel's correlation to correct the IPR curve below the bubble pressure for unfractured and *fractured* wells. However, there has not been a comprehensive investigation to ensure if the Vogel's correlation can be applied for fractured wells.

This paper presents a new correlation to build IPR curves or predict production performance below the bubble pressure for fractured wells. In order to investigate fractured well performance below bubble point, about 1,000 simulations runs were performed using well-refined size grid for several sets of relative permeability curves and PVT data. The simulation model has been validated against analytical solution. Those runs cover a big practical range of fracture penetration 0.1 to 1.0 and dimensionless fracture conductivities from 0.5 to 50. Steady state conditions were analyzed at this study. All the mechanisms that cause the difference between fractured well and radial flow performance below the bubble pressure has been also well studied and will be presented in this paper.

It was found that Vogel's correlation underestimates fractured well performance below bubble point. Vogel suggests a correction of AOF by 45% meanwhile the simulation results and new correlation show that the correction should be only 22%. Therefore, engineer could have an error of 43% using Vogel for estimating AOF for a fractured well.

Another finding of this study is that multiphase effect is dependent on fracture conductivity and almost independent on fracture penetration. Higher conductivity fractures has bigger gas banks therefore they are affected by multi-phase effect to greater extent than lower conductivity ones. The new correlation is now being used for different fields and better fits the data than Vogel's correlation.

Introduction

In 1968 Vogel[1] developed a correlation to estimate IPR curves for two-phase flow. Vogel's study was based on a numerical simulation, assuming radial flow, initial reservoir conditions at the bubble pressure, undamaged well and pseudo-steady state. In his simulations, Vogel used 4 sets of PVT and relative permeability data and showed that at those conditions AOF decreases 1.8 times due to multi-phase effect. However, Vogel's correlation is often used in a wider range of conditions than it was developed, including fractured wells, reservoirs above bubble pressure and steady-state flow. Vogel's deliverability curve is described by the following equation:

$$\frac{q_0}{q_{o,\max}} = 1 - 0.2\frac{p_w}{p_r} - 0.8\left(\frac{p_w}{p_r}\right)^2$$
$$q_{o,\max} = \frac{kh}{141.2\left[\ln(r_e/r_w) - 3/4 + s\right]} p_r \Big/ 1.8 \qquad (1)$$

Here $q_{o,\max}$ is the maximum possible flow rate (AOF), and q_o is the flow rate corresponding to wellbore flowing pressure p_{wf} and average reservoir pressure, p_r.

For damaged or stimulated wells, Standing[2] developed a modification to Vogel's correlation which uses flow efficiency as a parameter:

$$\frac{q_o}{q_{o,\max}^{FE=1}} = 1.8\,FE\left(1 - \frac{p_{wf}}{p_b}\right) - 0.8\,FE^2\left(1 - \frac{p_{wf}}{p_b}\right)^2 \qquad (2)$$

Note, that this equation is applicable only for values $p_{wf} \geq P_r\left(1 - \frac{1}{FE}\right)$ to avoid reversing effect on the IPR curve. Craft and Hawkins[3] presented the eqn (3) to calculate the absolute open flow rate.

$$\frac{q_{o,\max}}{q_{o,\max}^{FE=1}} = 0.624 + 0.376\,FE \qquad (3)$$

Many engineers use Vogel's equation, eqn 1, to correct production performance for fractured wells. It will be shown that below that Vogel undestimates the production behavior for fractured wells. Moreover, since a stimulated well can be considered as a well with negative skin (or efficiency, FE greater than 1), it is not uncommon that engineers apply eqn (1), or eqns (2) and (3) to estimate the IPR curve for fractured wells. As it will be shown below, this approach leads to overestimation of well performance.

In this work, a simulation study has been conducted in order to investigate the applicability of Vogel's IPR to fractured wells. The relative permeability curves and fluid properties that Vogel used, were also used in our simulation study. Additionally, the relative permeability and fluid properties of a major field in western Siberia-Russia was added to our set of data of our analysis. A big range of fracture penetrations and conductivities were considered in our study, simulating constant pressure boundary conditions or steady state.

IPR above P_b For Unfractured Wells

While evaluating an efficiency of production enhancement, it is very convenient to use IPR curves. To develop an analytical solution for IPR above the bubble point, the following equation could be used

$$q = \alpha_1 J_D \frac{k_o h}{\mu_o B_o}\left(p_r - p_{wf}\right) \tag{4}$$

where α_1 - constant dependant on unit system

J_D - dimensionless productivity index

The integral form of eqn (4) is as follows:

$$q = \alpha_1 J_D \, kh \int_{p_{wf}}^{p_r} \frac{k_{ro}}{\mu_o B_o} dp \tag{5}$$

Relative permeability can be considered constant above the bubble point, therefore, eqn (5) can be written as follows:

$$q = \alpha_1 J_D \, k k_{ro} h \int_{p_{wf}}^{p_r} \frac{1}{\mu_o B_o} dp \tag{6}$$

Correlations or approximations of the formation volume factor and viscosity can be used to obtain the final form of the eqn (6). However, taking the values of formation volume factor and viscosity at mid-point between average reservoir pressure and bottomhole pressure, eqn (4) can also be used. Figure 1 shows the formation volume factor, viscosity, relative permeability and mobility in the formation as function of the reservoir pressure. It can be seen in this plot that the mobility above the bubble point can be considered a straight line. This suggests that the average mobility ratio above the bubble point pressure can be evaluated at the mid-point between average reservoir pressure and bottomhole flowing pressure.

IPR below p_b For Unfractured Wells

The general IPR relationship for bottom flowing pressure below the p_b has the form of eqn (7), as follows:

$$q = \alpha_1 J_D \, kh \left[\int_{p_b}^{p_r} \frac{1}{\mu_o B_o} dp + \int_{p_{wf}}^{p_b} \frac{k_{ro}}{\mu_o B_o} dp \right], \quad p_{wf} < p_b \tag{7}$$

The second term in the equation is, in fact, the reason for "inefficient" behavior of IPR curve below p_b. Figures 1 and 2 below show the behavior of the mobility ratio below and above the bubble point. From this behavior it is clear that it is necessary to divide the mobility ratio integral into two to cover the range of the mobility ratio, from the bottom flowing pressure (below the bubble point) to the average reservoir pressure.

Fractured Model Description

A commercial black-oil numerical model was the one used for study a square reservoir of constant height with a fractured well producing in the center. Due to symmetry presented in our model, only one quarter of the reservoir was simulated. For the simulation, an irregular Cartesian grid was used in order to decrease simulation time and increase the accuracy of calculations. The fracture has been modeled as a number of cells with changed permeability and porosity. To simulate constant outer boundary pressure, to be able to reach steady-state, an infinite-conductivity big size oil reservoir connected to the opposite site of the fracture was modeled.

The fluid PVT properties and relative permeability curves that Vogel used for his research and an additional PVT and relative permeability set of data from a major western Siberian field, Figure 3, were used in our simulation study. End-point linear relative permeability curves were used for flow within fracture, see Figure 4. This end-point linear consideration is reasonable since linear type of relative permeability curves corresponds to a uniform distribution of pore sizes and proppant in the fracture is a very uniform rock. Non-Darcy flow was considered negligible within this study. The accuracy of the grid and the model was confirmed through comparisons of single-phase results with analytical solutions.

Construction of IPR Curves

A simulation run is performed with the fractured well producing at constant rate until steady-state is reached. Once the steady-state is reached, the bottom flowing pressure is recorded. This would give a point (q, p_{wf}) of the IPR curve. Many simulation runs are then conducted for a number of rates with the same well conditions to obtain the IPR curve for the specific fracture conditions (CfD and I_x) and for the specific PVT and relative permeability data. IPR curves are generated for different combinations of fracture penetration and fracture conductivity to evaluate the effect of CfD, and, I_x

on the IPR curves. The same procedure is followed for the different set of rock and fluid properties, Siberian's data and Vogel's. More simulations runs were performed with the data set from western-Siberia field than Vogel's. However, both provided very good representative amounts of runs to be use in the correlations.

Due to the gas-bank effect, the beginning of steady-state time is different for each combination of fracture conductivity and penetration. Therefore, for this study, the bottom flowing pressure for all the runs were taken at the same areal dimensionless time, t_{DA}, that is, the time at which the fracture with the highest conductivity reaches steady state (t_{DA}=0.138). IPR curves for the fluid and rock properties described above are presented in Figure 5. These curves were normalized by bubble point pressure and rate in order to compare the run results for different sets of data. Figure 6 presents the normalization of the IPR curves. As it can be seen in Figure 6, only the data below the bubble point pressure is presented in the plot.

Simulation Results

Results of simulations for different fracture length and conductivity at the same reservoir conditions are summarized in the Figure 5 and 6. It can be seen that the shape of the IPR dimensional curves depends on the fracture conductivity and penetration. However, once the IPR curves are normalized, all the IPR curves merge almost to a single curve.

Results of simulation of 5 PVT/Relative permeability data sets have been combined in order to build a correlation, which is suitable for fractured wells in the range of conductivities 0.5…50 and fracture half-lengths x_f = 100…500 meters. The correlation is presented is presented in eqn. (8).

$$\frac{q_o - q_b}{q_{o,\max} - q_b} = 1 - \left(0.73 - 0.041 Log\left(C_{fd}\right)\right)\frac{p_{wf}}{p_r} - \left(0.27 + 0.041 Log\left(C_{fd}\right)\right)\left(\frac{p_{wf}}{p_r}\right)^2$$

$$\frac{q_{o,noskin} - q_b}{q_{o,\max} - q_b} = 1.285 + 0.0347 Log\left(C_{fd}\right) \qquad (8)$$

Eqn (8) suggests that the lower fracture conductivities is, the straighter the curve is. The analysis also showed that the multi-phase correction does not depend greatly on fracture penetration but on fracture conductivity. The reason for this is that the fracture conductivity is what dictates how big the gas bank is created along the fracture. Figures 7 and 8 show the gas bank generated for I_x =0.3 and *CfD* of 0.1 and 5, respectively. When Figure 7 is compared with Figure 8, it can be seen that gas bank for a *CfD* of 0.1 is smaller than the gas bank for *CfD* of 1.0. This can be explained with the pressure profiles generated for the two different cases of fracture conductivity. The lower conductivity case has higher pressure drop inside the fracture (for the same rate case) and therefore the bubble pressure is reached closer to the wellbore than in the higher-conductivity case. Therefore, lower conductivity fractures would generate smaller bank effects.

Another average correlation was also determined following the same form as Vogel's correlation, without considering *CfD* as a parameter. Eqn. (9) gives the final form of the correlation, providing an error no greater than 5% for the same range of fracture conductivities.

$$q_o = q_b + \frac{J_D p_r}{1.31}\left[1 - 0.65\frac{p_{wf}}{p_b} - 0.35\left(\frac{p_{wf}}{p_b}\right)^2\right] \qquad (9)$$

Comparing Eqn (9) with Vogel's, it can be seen that Vogel's correlation underestimates fractured well performance below bubble point. Vogel suggests a correction of AOF by 45% meanwhile the simulation results (and Eqn (9)) show that the correction should be only 22%. Therefore, engineer could have an error of 43% using Vogel for estimating AOF for a fractured well. Figure 6 shows the above remarks.

Additionally, eqn (9) is compared with the Vogel-Standing correlation for two cases: a *CfD* of 0.5 and I_x of 0.1, and a *CfD* of 2.0 and I_x of 0.3. For this comparison, the flow efficiency was calculated from the *CfD* and I_x, and then IPR was determined using Vogel-Standing correlation. Figures 9 and 10 show the results of this comparison. It can be seen that Vogel-Standing correlation overestimates very much the IPR curves, to the point that makes the Standing correlation completely invalid for fractured wells.

Let us review now the production mechanisms that would explain less multiphase effect in fractured wells compared to radial-flow unfractured wells. It is known that fractured wells have a different flow pattern due to the rock properties differences between the fracture and the formation (difference in conductivity). In order to understand more the multiphase flow effect in the fractured wells, two main factors were analyzed. First, the mechanisms for the fact of having different relative permeability curves in the fracture than in the formation. Secondly, the effect of reduction of the effective permeability around the fracture due to the increase of gas saturation.

The mobility behavior inside the fracture (using end-point-linear relative permeabilities) is presented in Figure 2. Note the difference in fluid mobility below the bubble point pressure compared to the mobility behavior in the formation as shown in Figure 1. In Figure 2, it can be seen that below the bubble point pressure the mobility decreases almost linearly at slower pace than the mobility in the formation (comparing Fig 2 and Fig. 1). This implies that below bubble point, the relative permeability or multiphase effect in the fracture is much less than the effect in the formation. Moreover, it can be seen that gas saturation in the fracture is very small compared to the one in the formation. Therefore, the fracture provides a very conductive way for gas to escape from nearby formation and keeping relatively low gas saturation in the fracture and even in the formation (if it would be compared to radial model).

Secondly, Holditch[4] and many other authors have shown that the production of a fractured well is not highly affected by permeability reduction at the fracture face or fracture face skin. One of the main reasons is that the fluid velocity across

the fracture is a lot lower than in radial well model and the pressure drop is directly proportional to the velocity. However, it has also been shown that if the damage around the fracture is too deep, it could have significant production impairment. In our case, the gas bank generates is big enough to create some production impairment but not enough to be the same as in an unfractured well.

Conclusions

The following conclusions can be drawn from this work:

1. Two new correlations to build IPR's curves or predict production performance for fractured wells below the bubble point pressure were presented in this paper.
2. Vogel's correlation underestimates fractured well performance below bubble point. Vogel suggests a correction of AOF by 45% meanwhile the simulation results and new correlation show that the correction should be only 22%.
3. Multiphase effect is dependent on fracture conductivity and almost independent on fracture penetration. Higher conductivity fractures has bigger gas banks therefore they are affected by multiphase effect to greater extent than lower conductivity fractures.
4. Vogel-Standing correlation over-estimates the IPR curve for fractured well if equivalent flow efficiency, FE, is calculated from a fracture conductivity and penetration.

Nomenclature

t_{DA} = Dimensionless time based on drainage area

r_w = Wellbore radius (m)

r_e = Drainage radius (m)

J_D = Dimensionless Productivity Index

B_o = Oil formation volume factor, (rm^3/sm^3)

C_{fD} = Dimensionless fracture conductivity

FE = Flow efficiency, (dimensionless)

h_f = Fracture height, (m)

I_x = Fracture penetration, (dimensionless)

k = Formation permeability, (mD)

k_f = Proppant or fracture permeability, (mD)

k_o = Effective permeability to oil, (mD)

k_{rg} = Relative permeability to gas, (dimensionless)

k_{ro} = Relative permeability to oil, (dimensionless)

N_p = Proppant number, (dimensionless)

p_b = Bubble point pressure, (bar)

p_r = Average reservoir pressure, (bar)

p_{wf} = Wellbore flowing pressure, (bar)

q_b = Oil flow rate at $p_{wf} = p_b$, (sm^3/day)

q_o = Oil flow rate, (sm^3/day)

$q_{o,max}$ = absolute open flow, (sm^3/day)

$q_{o,no\ skin}$ = flow rate with no multiphase effect, (sm^3/day)

s = Skin factor (dimensionless)

w_f = Fracture width, (m)

x_f = Fracture-half length (m)

μ_o = Oil viscosity, (cp)

Acknowledgements

The authors thank YUKOS E&P management for allowing publishing this paper.

References

1. Vogel J. V.: "Inflow Performance Relationships for Solution-Gas Drive Wells", *Trans.*, AIME (1968) 243, 83-92.
2. Standing, M.B. "Inflow Performance Relationships for Damaged Wells Producing by Solutions-Gas Drive", *Journal of Petroleum Technology* (November 1970) 1399-1400.
3. Craft B. C., Hawkins M.: "Applied Reservor Engineering", Englewood Clieffs, NJ: Prentice Hall, 1975.
4. Holditch, S.A.:"Factors Affecting Water Blocking and Gas Flow from Hydraulically Fractured Gas Wells," *Journal of Petroleum Technology* (December 1979b) 31, No.12, 1515-1524.

Si Metric Conversion Factors

bbl	*	1.589 873	E-01	=	m^3
ft	*	3.048	E-01	=	m
psi	*	6.984 757	E+00	=	kPa

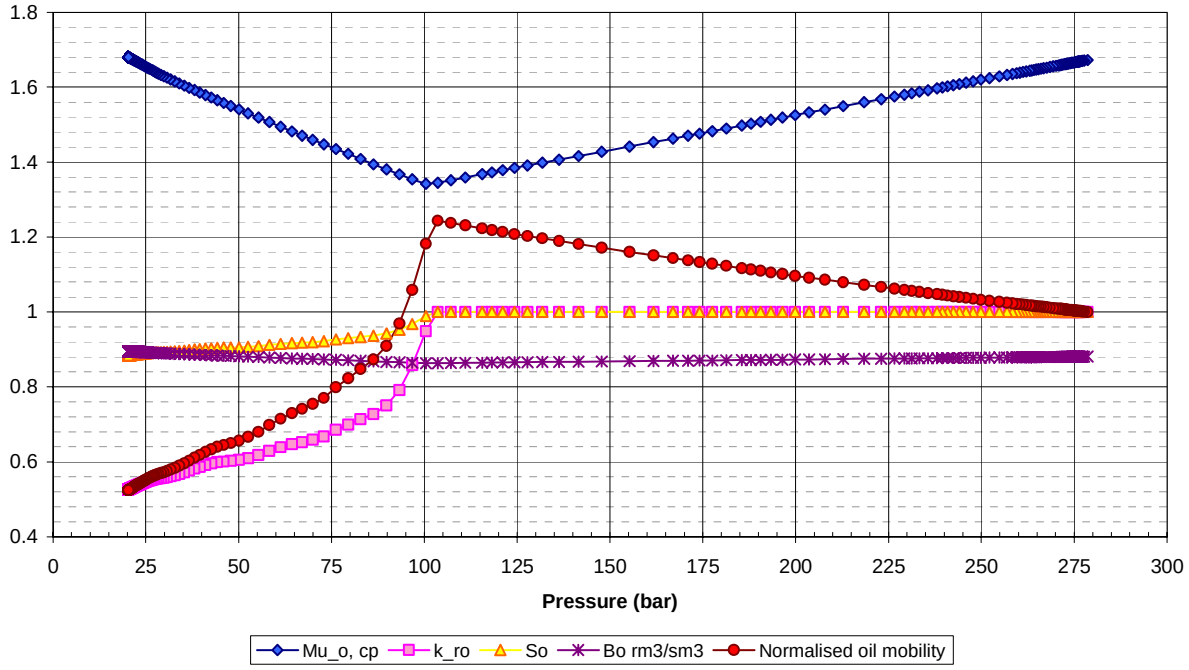

Figure 1 - Fluid mobility vs pressure (reservoir rock)

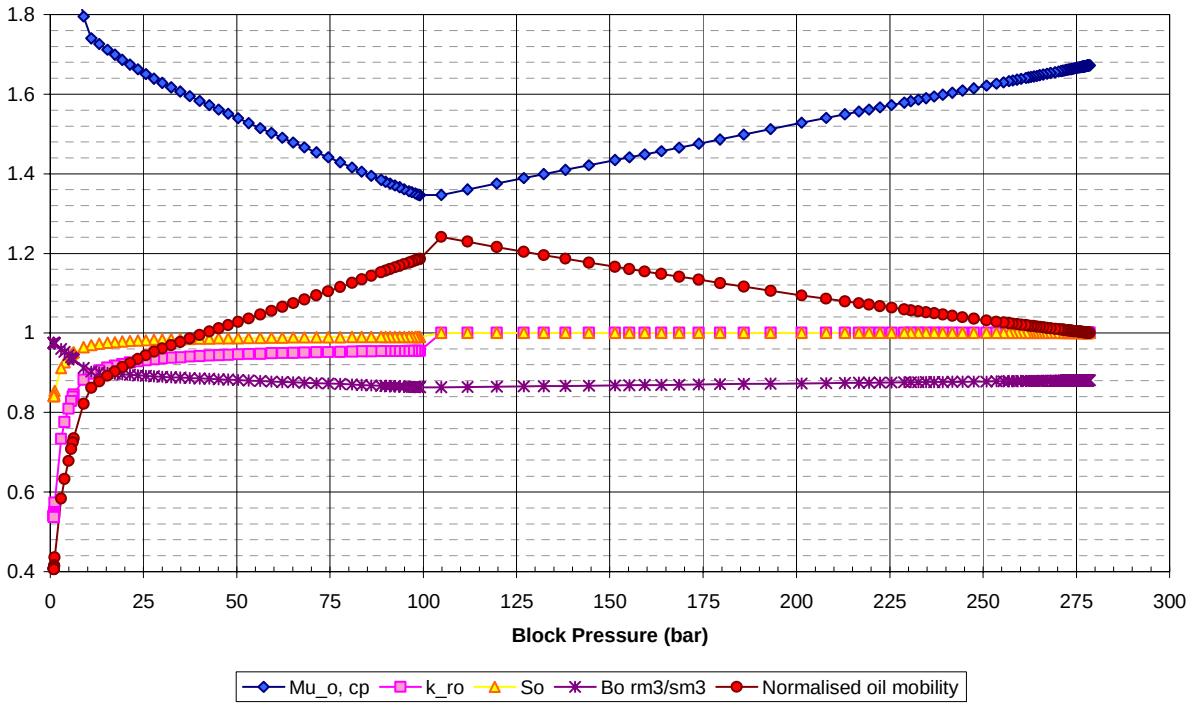

Figure 2 - Fluid mobility VS pressure (within the fracture)

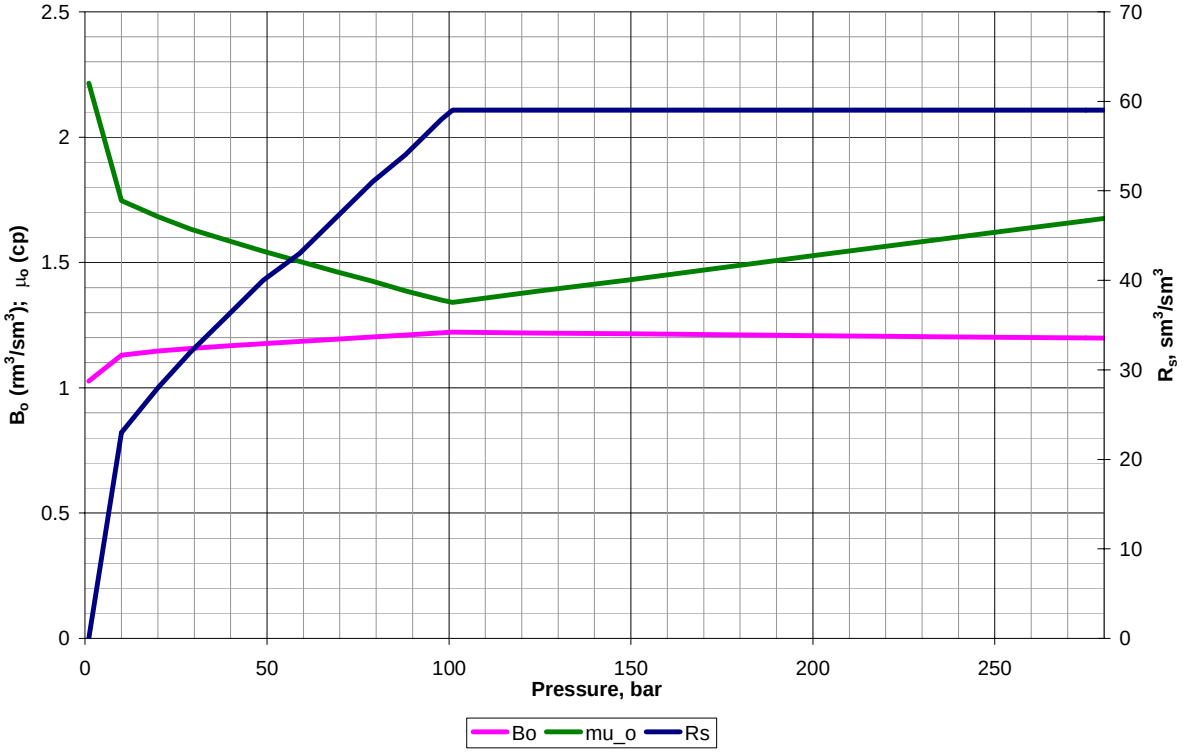

Figure 3 - PVT curves for the major western Siberia field used in analysis

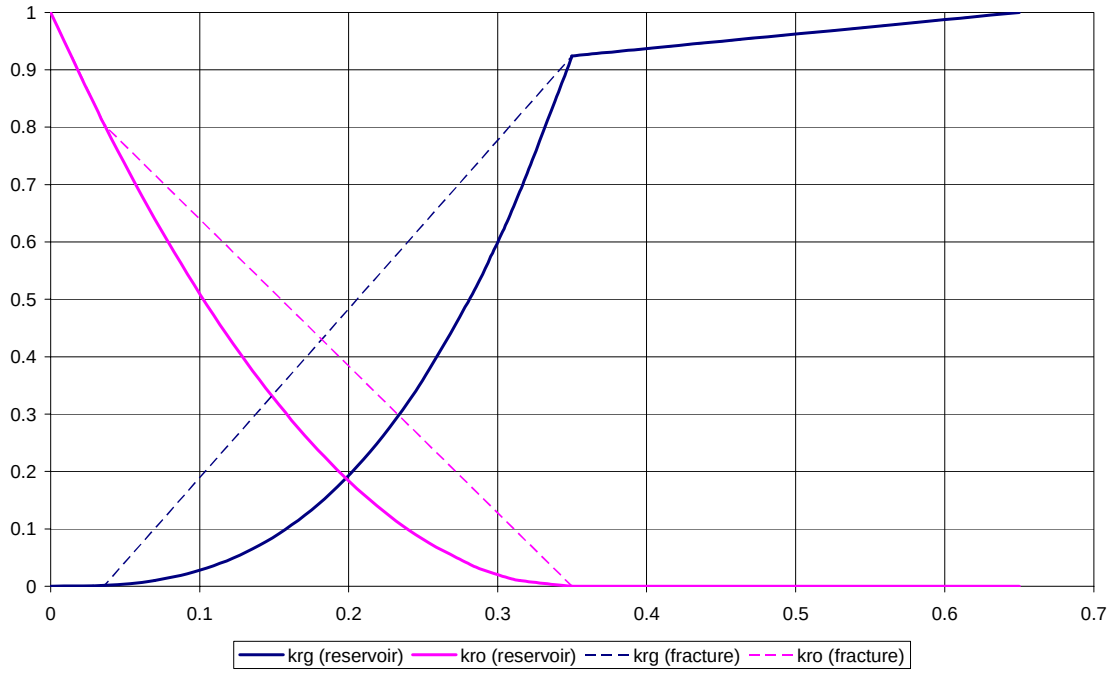

Figure 4 - Relative permeability curves for the major Western Siberia field

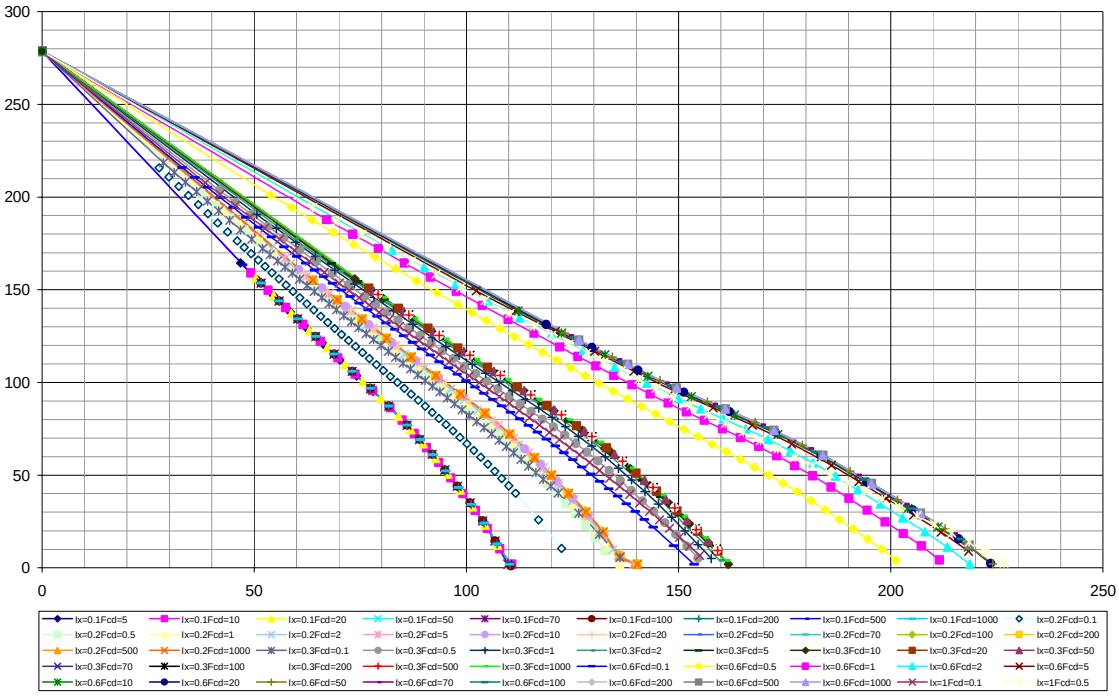

Figure 5 – IPR curves results from the simulation

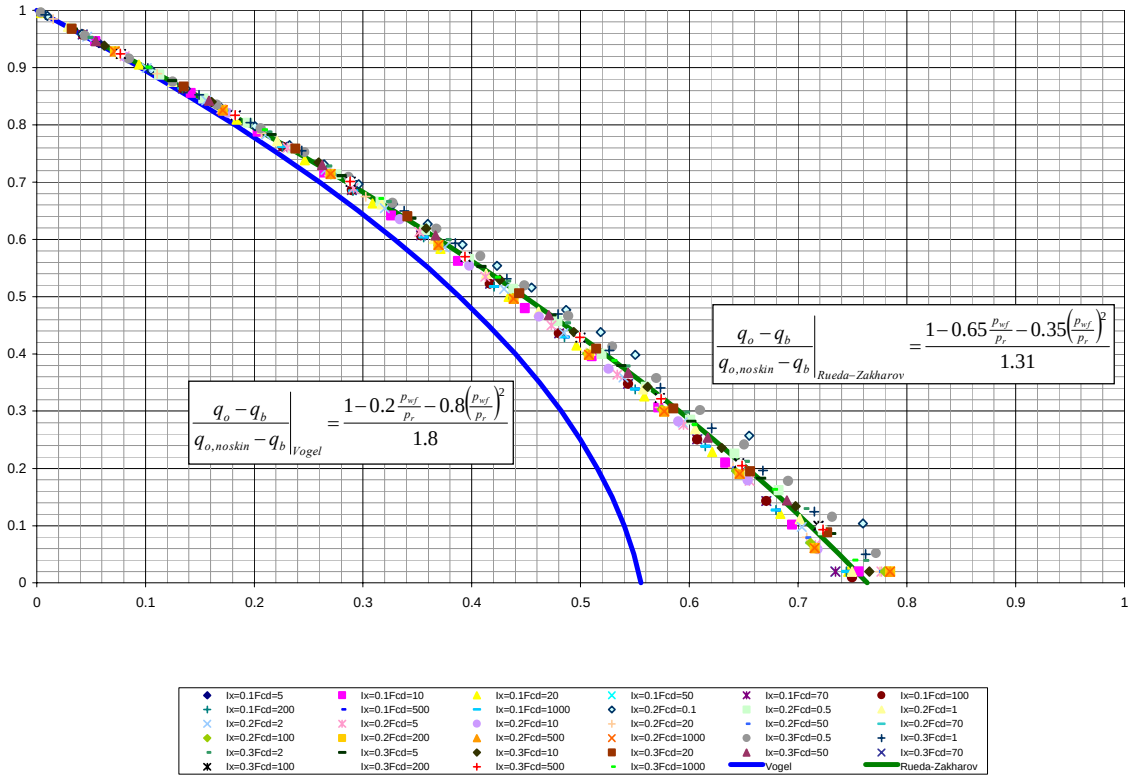

Figure 6 - Simulation results normalized by p_b and $q_{o,\ no\ skin}$ (only points below p_b are shown)

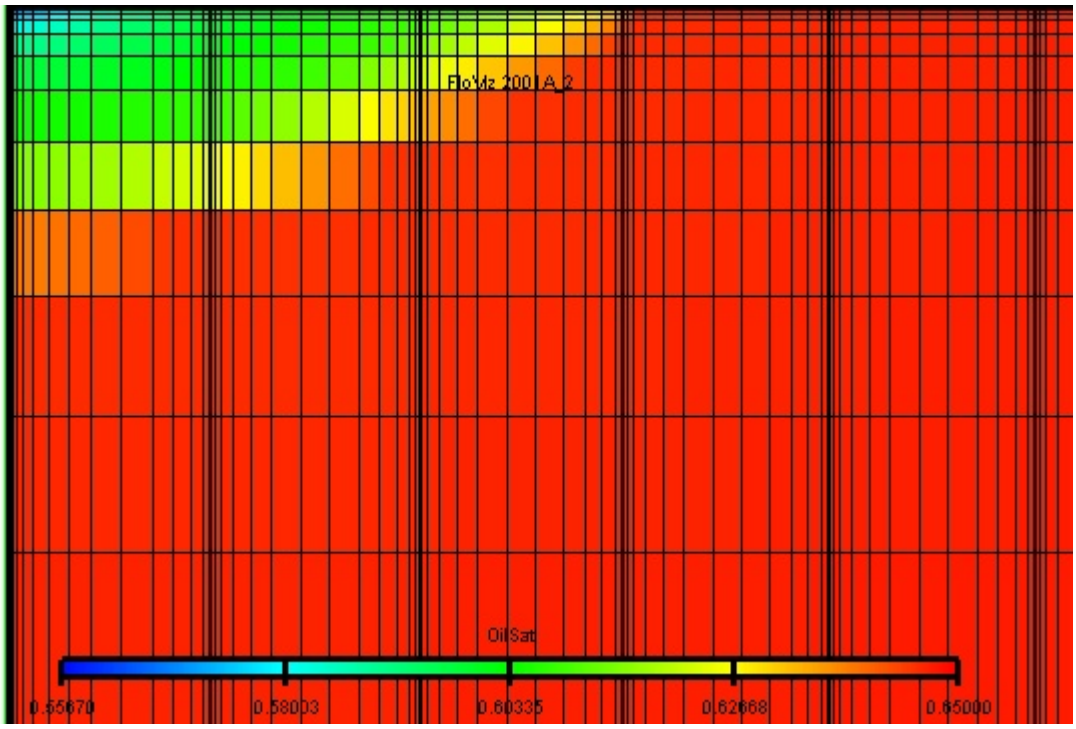

Figure 7 - Gas bank generated for a fractured well of I_X = 0.3 and C_{fD} = 0.1

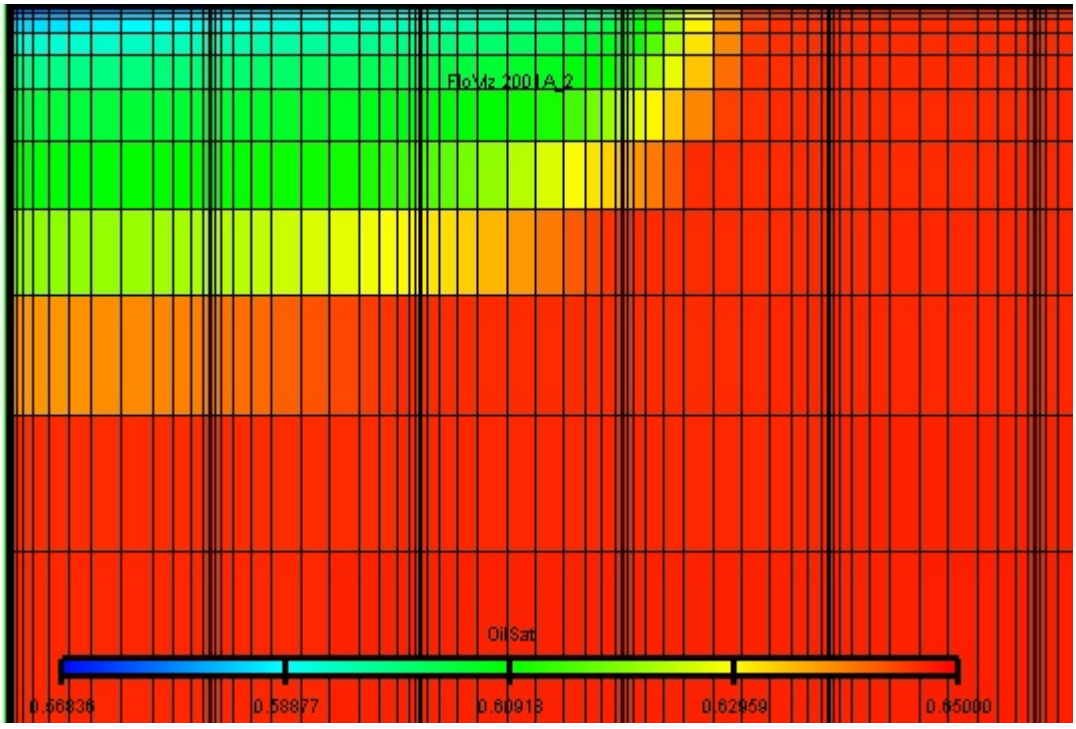

Figure 8 - Gas bank generated for a fractured well of I_X = 0.3 and C_{fD} = 1.0

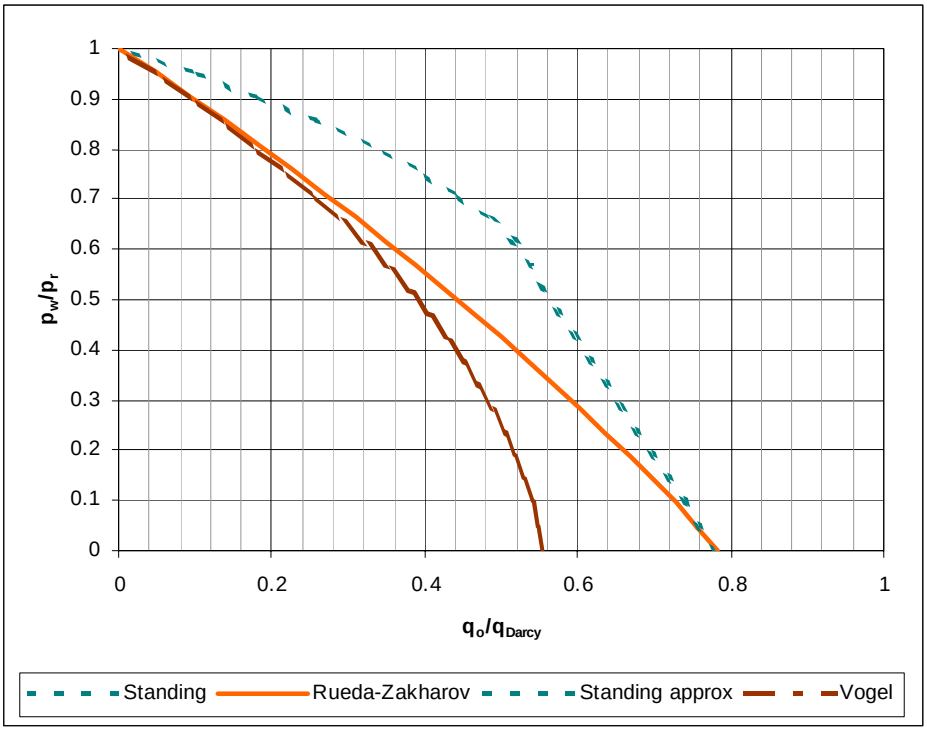

Figure 9 – Comparison of Vogel-Standing vs Rueda-Zakharov's correlations for Ix=0.1 and Cfd=0.5

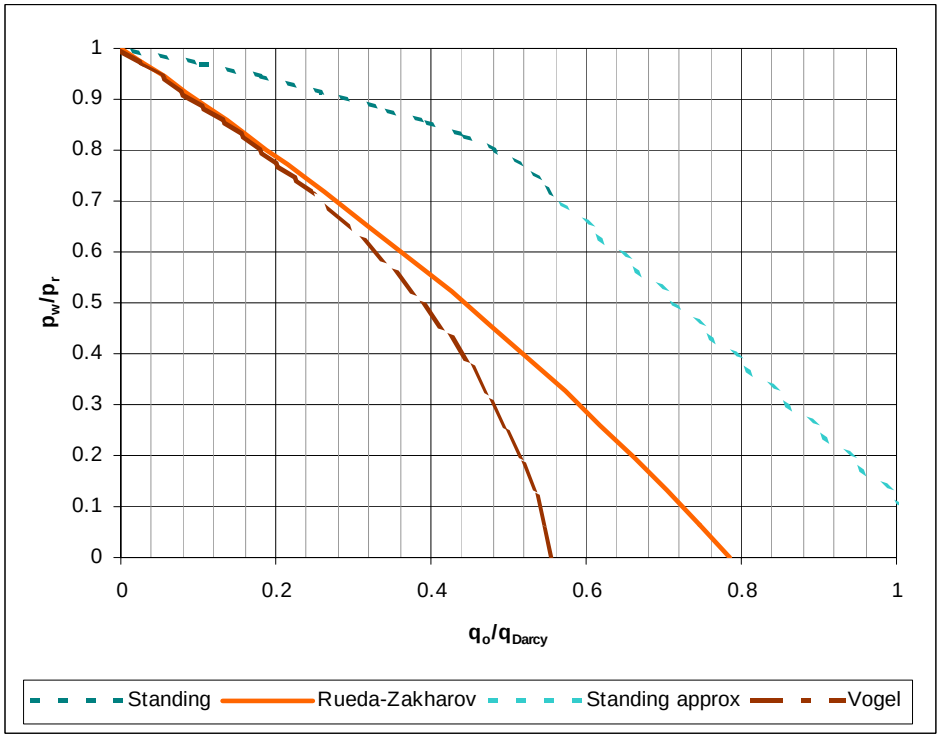

Figure 10 – Comparison of Vogel-Standing vs Rueda-Zakharov's correlations for Ix=0.1 and Cfd=2.0